White, D. J., Cheuk, C. Y. & Bolton, M. D. (2008). *Géotechnique* **58**, No. 10, 771–779 [**doi:** 10.1680/geot.2008.3692]

The uplift resistance of pipes and plate anchors buried in sand

D. J. WHITE*, C. Y. CHEUK† and M. D. BOLTON‡

The design of buried anchors and pipelines requires assessment of the peak uplift resistance. This paper describes a limit equilibrium solution for the uplift resistance of pipes and plate anchors buried in sand. The geometry of this solution reflects observations from model tests. Peak angles of friction and dilation are found using established correlations that capture the influence of stress level and density. These angles govern the geometry of the failure mechanism and the mobilised resistance. The solution is validated using a database of 115 model tests on pipes and strip anchors assembled from the published literature. Good agreement with the overall database is shown, without optimisation of any input parameters. The method overpredicts the uplift resistance of smooth model pipes by ~10%, highlighting the influence of pipe roughness. In contrast, it is shown that the solution for uplift resistance based on the limit theorems of plasticity is generally unconservative. The assumption of normality, which is required by the limit theorems, leads to an unrealistic failure mechanism involving uplift of a far wider zone of soil than is seen in model tests. Plasticity theory, with normality, is inappropriate for modelling this class of kinematically restrained problem in drained conditions, as normality is not observed. As finite element analysis is not routinely used in practice—partly owing to the difficulty in selecting appropriate input parameters to describe dilatancy and plastic flow—the simple analytical idealisation described in this paper provides a useful tool for uplift resistance prediction. Simple charts for the prediction of peak uplift resistance from critical state friction angle, relative density and normalised burial depth are presented, to aid the design of buried pipes and anchors.

KEYWORDS: anchors; centrifuge modelling; design; model tests; sands

La configuration d'ancrages et de canalisations enterrés nécessite l'évaluation de la résistance de pointe au soulèvement. La présente communication décrit une solution d'équilibre limite pour la résistance au soulèvement de canalisations et de plaques d'ancrage fixées dans le sable. La géométrie de cette solution reflète des observations de tests modèles. Des angles de pointe de la friction et de la dilatation sont établis par l'établissement de corrélations capturant l'influence du niveau de contrainte et de la densité. Ces angles déterminent la géométrie du mécanisme de rupture et de la résistance mobilisée. La solution est validée en utilisant une base de données de 115 essais sur modèle effectués sur des canalisations et des dispositifs d'ancrage assemblés conformément aux documents publiés. On démontre une bonne conformité avec la base de données générale, sans optimisation de paramètres d'entrée. La méthode prédit par excès de l'ordre de ±10% la résistance au soulèvement de canalisations lisses, en mettant en lumière l'influence de la rugosité des canalisations. Par contraste, on démontre que la solution à la résistance au soulèvement basée sur des théorèmes limites sur la plasticité est généralement extrême. L'hypothèse de la normalité, que nécessitent les théorèmes limites, engendre un mécanisme de rupture non réaliste comportant le soulèvement d'une zone de sol beaucoup plus large que celle des tests sur modèle. La théorie de la plasticité, avec normalité, ne convient pas pour la modélisation de cette classe de problème à modération cinématique dans des conditions drainées, étant donné que l'on ne relève pas de normalité. Étant donné que, dans la pratique, on n'utilise pas l'analyse aux éléments finis, en partie du fait de la difficulté de la sélection de paramètres d'entrée appropriés pour la description de la dilatance et de l'écoulement plastique, l'idéalisation analytique simple décrite dans la présente communication constitue un outil utile pour prédire la résistance au soulèvement. La communication présente de simples tableaux pour la prédiction de la résistance extrême au soulèvement à partir de l'angle de friction à l'état critique, du poids spécifique et de la profondeur d'enterrement normalisée, pour faciliter l'étude d'ancrages et de canalisations enterrés.

INTRODUCTION

Engineering structures may be subjected to uplift forces originating from sources such as wind load or wave action. A common method to obtain the required stabilising force is to bury a plate anchor in soil that is fixed to the structure through a tie rod. Installation of these buried anchors normally involves excavation and back-filling. The anchors transmit upward forces directly from the anchored structure to the soil, through mobilisation of uplift resistance provided by the soil cover. This type of foundation is widely used for transmission towers and in marine mooring operations.

The uplift resistance of buried pipes is a critical parameter in the design of offshore pipelines used for oil transportation. In order to ease the flow and prevent the solidification of wax fractions, it is necessary to transport the oil at high temperature and pressure. These extreme operating conditions cause thermal expansion, which may lead to axial compressive stresses in the pipe if such expansion is restrained by axial friction and end fixity. The pipeline is then vulnerable to relief of these axial stresses through upward or lateral thermal buckling. Trenching and backfilling is often used to provide vertical restraint against

Manuscript received 1 March 2006; revised manuscript accepted 13 August 2008.
Discussion on this paper closes on 1 June 2009, for further details see p. ii.
* Centre for Offshore Foundation Systems, University of Western Australia, Perth, Australia.
† Department of Civil Engineering, University of Hong Kong.
‡ Department of Engineering, University of Cambridge, UK.

Delivered by ICEVirtualLibrary.com to:
IP: 129.169.110.8
On: Tue, 02 Aug 2011 16:19:32

buckling. For design, the available uplift resistance must be predicted.

This wide range of applications has attracted significant research attention, focused on predicting the uplift resistance of buried objects. A large database exists as a result of a number of experimental studies. Various prediction formulae based on an assumed failure mechanism have also been proposed (e.g. Vermeer & Sutjiadi, 1985; Trautmann *et al.*, 1985; Murray & Geddes, 1987). More rigorous solutions based on plasticity theory have been presented by Merifield *et al.* (2001) and Merifield & Sloan (2006). These various prediction methods, based on different assumed failure mechanisms, stress distributions and material behaviour, can lead to very different results.

OBJECTIVES

The purpose of this paper is to present the validation of a simple limit equilibrium solution for the vertical pullout resistance of pipes and plate anchors buried in sand. The limit equilibrium solution is inspired by the deformation mechanisms observed in model tests (Cheuk *et al.*, 2007). Peak angles of friction and dilation that vary with stress level and density are used, following Bolton (1986), in order to establish the geometry of the mechanism, and the resistance mobilised on the failure planes. The solution is shown to provide good agreement with a large database of model tests results that has been assembled from the published literature. Simple design charts are presented. It is shown that plasticity solutions for an ideal frictional material (which exhibits normality) can be unconservative. Finite element solutions with a non-associated flow rule can give closer predictions. However, finite element analysis is not routinely used in practice, and simple analytical idealisations of the kind described in this paper remain the principal tool used by designers.

UPLIFT RESISTANCE PREDICTION MODELS

The geometry and nomenclature of this boundary value problem are defined in Fig. 1(a), for the case of a pipe of diameter D, and in Fig. 1(b) for a strip anchor of breadth B. The cover depth H is measured to the waist of the pipe, and the uplift resistance per unit length is denoted P. A number

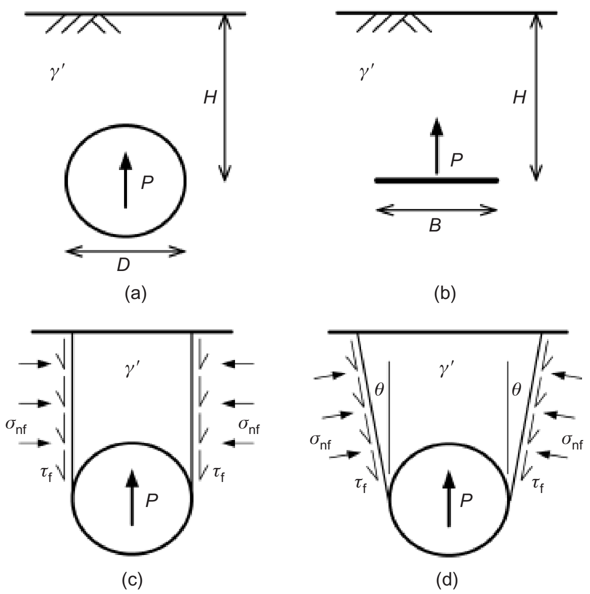

Fig. 1. Pipe and strip anchor uplift geometry and simple failure mechanisms: (a) pipe geometry; (b) strip geometry; (c) vertical slip mechanism; (d) inclined slip mechanism

of theoretical models for predicting uplift resistance are available. These solutions can be broadly classified into two categories: limit equilibrium and plasticity solutions. The limit equilibrium approach does not impose any particular flow rule, but instead allows the equilibrium of any assumed failure mechanism to be assessed. It is necessary to assume the stress distribution in the soil, so this assumption must be realistic if an accurate solution is to be reached.

Two widely adopted mechanisms for pipe uplift resistance are illustrated in Figs 1(c) and 1(d). The vertical slip model assumes that failure occurs along a pair of straight slip planes, which initiate from the pipe waist and extend to the soil surface (Fig. 1(c)). The uplift resistance arises from the weight of the lifted block and the shear stress on the slip planes. An alternative is to orient the slip planes at some inclination θ to the vertical (Fig. 1(d)). In this case, the uplift resistance is equal to the lifted soil weight plus the resultant vertical force on the slip planes, which arises from both the shear and the normal stresses.

Plasticity solutions based on lower- and upper-bound limit analysis are more rigorous than limit equilibrium solutions, providing definite limits on the true solution, albeit for a particular class of material. This material must obey normality, which is rarely observed during drained failure of soil. For the uplift problem, the most simple kinematically admissible mechanism leads to an upper-bound solution as shown in Fig. 1(d). Normality requires that the shear surfaces be inclined at the angle of dilation ψ to the direction of pipe movement, where the dilation and friction angles are identical (i.e. $\theta = \psi = \phi$ in Fig. 1(d)). In a frictional material obeying normality there is no dissipation during shear or on sliding planes, so the uplift resistance is simply the weight of the lifted soil. Hence, from the area of the trapezium of soil above the pipe, the uplift resistance is given by

$$\frac{P}{\gamma' HD} = N_\gamma = 1 + \frac{H}{D}\tan\phi \tag{1a}$$

By idealising the pipe as a flat horizontal element, a small additional volume of soil is considered, occupying the space that is actually filled by the top half of the pipe. This discrepancy is small, and allows equation (1a) to be compared with solutions for plate anchors. However, at shallow embedments (low H/D), equation (1b), which accounts for the circular surface of the pipe, is preferable.

$$\frac{P}{\gamma' HD} = N_\gamma = 1 - \frac{\pi D}{8H} + \frac{H}{D}\tan\phi \tag{1b}$$

Vermeer & Sutjiadi (1985) used the same upper bound in the analysis of buried anchors. Merifield *et al.* (2001) and Merifield & Sloan (2006), using finite element limit analysis, generated upper- and lower-bound solutions for the uplift resistance of plate anchors that are essentially identical to equation (1). For this kinematically constrained problem, the upper bound given by Fig. 1(d) cannot be improved through numerical techniques. However, model test observations described below indicate that this upper-bound solution is not representative of the true failure mechanism, and can lead to poor prediction of the uplift resistance.

In addition to limit equilibrium and plasticity solutions, numerical studies of uplift resistance have been conducted. Rowe & Davis (1982) described a comprehensive finite element study of the breakout resistance of buried anchor plates. The soil was assumed to have a Mohr–Coulomb failure criterion, and both associated and non-associated flow rules were adopted. Their results, expressed as N_γ in the form of simple charts, suggest that soil dilatancy can significantly increase the ultimate anchor capacity at moderate depth ($H/D > 3$) in medium to dense sand ($\phi > 30°$).

Delivered by ICEVirtualLibrary.com to:
IP: 129.169.110.8
On: Tue, 02 Aug 2011 16:19:32

However, the effects of the initial stress state and anchor roughness are less important.

MODEL TEST OBSERVATIONS

Cheuk *et al.* (2007) presented the results of a series of model tests that aimed to establish the failure mechanism during uplift of a pipe buried in dry sand. Image analysis was used to convert the observed deformation into detailed measurements of the failure mechanism. Previous model tests have suggested that the uplift response of buried pipes and buried plate anchors are similar (Dickin, 1994). The observations are therefore likely to apply to either case. Cheuk *et al.* (2007) tested a model pipe section with a diameter D of 0·1 m, which was extracted from an initial embedment H of 0·3 m at an upward velocity of 10 mm/h. The slow movement allowed regular photography of the soil deformation using a pair of digital cameras. The displacement field was subsequently deduced using particle image velocimetry (PIV) and photogrammetry (White *et al.*, 2003). A total of four tests were conducted on Leighton Buzzard silica sands of two different grain sizes (D_{50} = 0·28 mm and 2·24 mm) at two different relative densities I_D of ~30% and ~90%. The two sands share the same critical state friction angle ϕ_{crit} of 32° as measured in direct shear box tests.

Figure 2(a) shows the velocity field when the peak resistance is mobilised in one of the tests involving dense coarse sand. The failure mechanism resembles an inverted trapezoid bounded by a pair of distributed shear zones (A). The width of the shear zone increases towards the soil surface with a small outward curvature. This is presumably due to the increase in dilation angle with reducing stress level near the ground surface. Limited downward soil movement was observed near the pipe waist. This indicates that a complete flow-round mechanism was not present at the moment of peak uplift. Instead, the flow-round mechanism was mobilised after significant additional pipe movement, and is not relevant to the prediction of peak uplift resistance.

An alternative way of presenting the failure mechanism is shown in Fig. 2(b), in which the horizontal profiles of the vertical soil velocity of all the four tests are plotted. The sloping parts of the profiles correspond to the mobilised shear zones. The inclination of the shear zone was found to be dependent on the soil density, but less affected by particle size. In dense conditions the shear zone was more inclined, indicating greater dilation (B) compared with loose soil (C). The inclination of the shear zones to the vertical is in the range 6–20°. If this mechanism is idealised as a single shear plane, this would imply a dilation angle of 6–20°, which is much smaller than the friction angle of the deforming soil. For the tested soils $\phi_{crit} = 32°$, whereas Bolton's (1986) flow rule suggests a peak friction angle as high as 39° at a stress level of the order of 10 kPa, even at the lowest tested relative density of 30%. This contrast, between the observed failure mechanism and the failure mechanisms required by classical plasticity to satisfy normality, brings into question the reliability of the predicted uplift resistance.

The deformation measurements presented by Cheuk *et al.* (2007) are sufficiently detailed to prove that normality is violated through energy considerations. In a purely frictional material such as dry sand there is no internal dissipation if normality is obeyed, as the vector product of the stress and strain increment vectors is zero. Therefore the only work done within an upper-bound solution is against self-weight. However, in these experiments, at peak resistance the rate of work done lifting the pipe exceeded the rate of potential energy gain within the soil mass by a factor of ~1·8. This factor was found by integrating the incremental vertical velocity throughout the volume of the deforming soil. There was therefore significant energy dissipation within the soil, in contravention of normality.

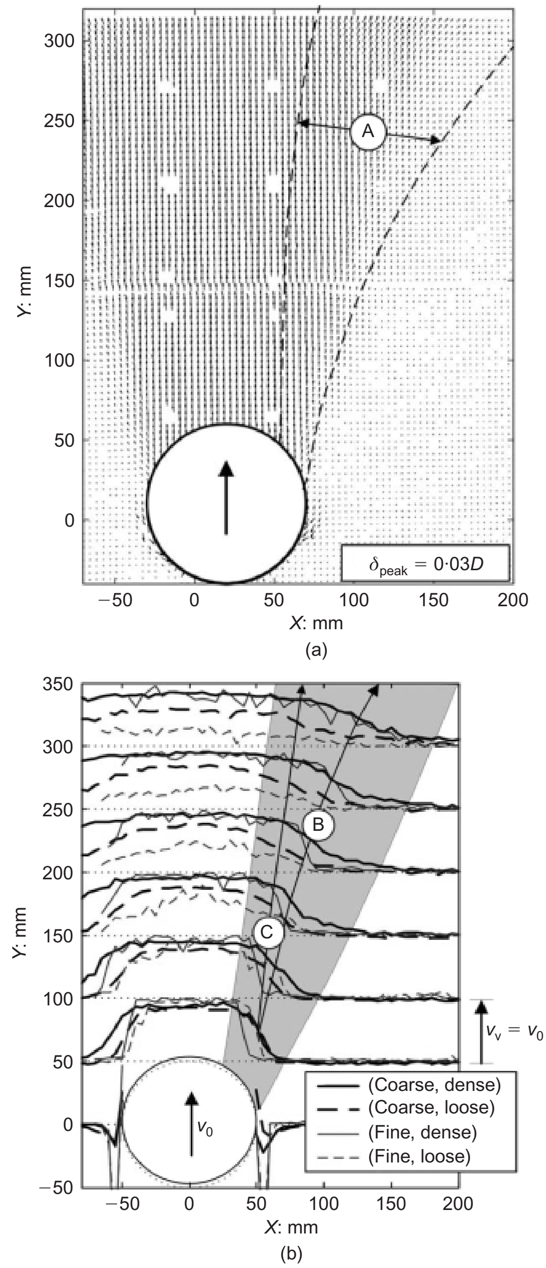

Fig. 2. Observed deformation mechanism at peak uplift resistance (Cheuk *et al.*, 2007): (a) incremental displacement field; (b) vertical velocity profiles

LIMIT EQUILIBRIUM SOLUTION

Given the experimental evidence that normality does not hold, the attractive rigour of the bound theorems may be of limited value for this class of boundary value problem. Instead, the following limit equilibrium solution is used for the prediction of peak uplift resistance. Although limit equilibrium solutions lack the apparent rigour of the bound theorems, they have the advantage that normality can be neglected, the assumed failure mechanism can be tuned to match experimental observations, and alternative flow rules to link strength and dilatancy can be introduced.

This solution assumes that an inverted trapezoidal block is lifted above the pipe. The shear planes on each side of the block are inclined at the angle of dilation (i.e. $\theta = \psi$ in

Delivered by ICEVirtualLibrary.com to:
IP: 129.169.110.8
On: Tue, 02 Aug 2011 16:19:32

Fig. 1(d)). The uplift resistance is equal to the weight of the lifted soil block plus the shear resistance along the two inclined failure surfaces. Calculation of the weight of the block is straightforward, but an assumption regarding the distribution of normal stress (and hence shear resistance) along the slip planes must be made. It is assumed that the normal stress on the sliding planes is equal to the in situ value inferred from K_0 conditions using the small Mohr's circle shown in Fig. 3. As a result, a realistic increase in vertical stress ahead of the pipe is permitted, as shown by the larger Mohr's circle representing the conditions at peak resistance. From the geometry of these two Mohr's circles, the peak mobilised shear stress along the slip surface can be calculated as

$$\tau = \gamma' z \tan\phi_{\text{peak}}\left[\frac{(1+K_0)}{2} - \frac{(1-K_0)\cos 2\psi}{2}\right] \tag{2}$$

By integrating along the slip planes and equating the vertical forces acting on the sliding block, the peak uplift resistance per unit length, P, is calculated as

$$P = \gamma' HD + \gamma' H^2 \tan\psi + \gamma' H^2 \left(\tan\phi_{\text{peak}} - \tan\psi\right) \times \left[\frac{(1+K_0)}{2} - \frac{(1-K_0)\cos 2\psi}{2}\right] \tag{3}$$

An additional term $(-\pi\gamma' D^2/8)$ applies for a pipe, as per the difference between equations (1a) and (1b). Equation (3) can be normalised to give a dimensionless factor N_γ, which is a function of the depth–diameter ratio (H/D) and an uplift factor F_{up}:

$$\frac{P}{\gamma' HD} = N_\gamma = 1 + F_{\text{up}}\frac{H}{D} \tag{4(a)}$$

$$\frac{P}{\gamma' HD} = N_\gamma = 1 - \left(\frac{\pi}{8}\frac{D}{H}\right) + F_{\text{up}}\frac{H}{D} \tag{4(b)}$$

where equation (4a) corresponds to a strip anchor, equation (4b) corresponds to a pipe, and

$$F_{\text{up}} = \tan\psi + \left(\tan\phi_{\text{peak}} - \tan\psi\right)\left[\frac{1+K_0}{2} - \frac{(1-K_0)\cos 2\psi}{2}\right] \tag{5}$$

This limit equilibrium solution includes three independent variables related to the soil: (a) the peak friction angle ϕ_{peak}; (b) the dilation angle ψ; and (c) the effective soil unit weight γ'. If normality is invoked, such that $\phi_{\text{peak}} = \psi$, equation (3) reduces to the simple upper-bound solution given by equation (1).

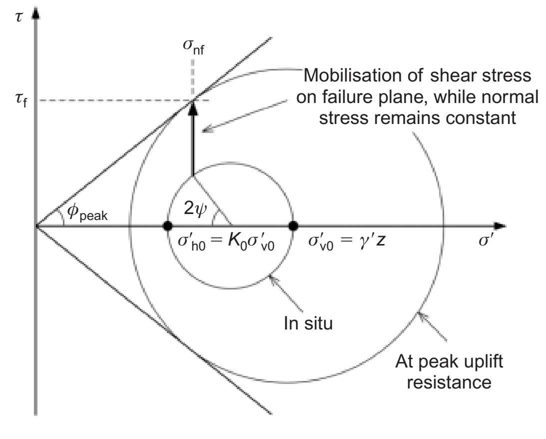

Fig. 3. Assumed Mohr's circles in situ and at peak uplift resistance

To use equation (5) it is necessary to estimate the friction and dilation angles, noting that these vary with density and stress level. Bolton (1986) proposed simple correlations to link dilation angle to relative density I_D and grain-crushing strength σ_c, relative to the mean effective stress p' (equations (6) and (7)). Furthermore, element tests show that the peak dilation angle during shear is approximately 1·25 times the difference between ϕ_{peak} and ϕ_{crit} (Bolton, 1986). This is in agreement with Rowe's stress dilatancy law (Rowe, 1962, 1969), and in contrast with normality. These correlations allow the limit equilibrium solution to be recast in terms of I_D and ϕ_{crit}, which are more easily determined during a site investigation.

Limits of 0 and 4 apply to the relative dilatancy index I_R given by equation (7), and the value of the parameter m is to be taken as 3 under triaxial strain or 5 in the plane-strain conditions appropriate for pipe uplift. Randolph *et al.* (2004) report values of Q, the natural logarithm of the grain-crushing strength, σ_c and ϕ_{crit} for a variety of sands, which are summarised in Table 1.

$$\phi_{\text{peak}} - \phi_{\text{crit}} = 0{\cdot}8\psi_{\text{peak}} = mI_R \tag{6}$$

$$I_R = I_D(Q - \ln p') - 1 = I_D \ln\left(\frac{\sigma'_c}{p'}\right) - 1 \tag{7}$$

Bolton's correlations allow the limit equilibrium solution to capture the influence of dilatancy on the geometry of the failure mechanism, and therefore the shearing resistance and overburden weight that oppose uplift. As the shear planes in the solution are straight, a single representative dilation angle is required, and a single representative mean effective stress at failure, p', must be assumed. This value of p' has been taken as the effective overburden at the pipe waist, $\gamma' H$. The selection of p' at pipe waist instead of the mid-depth between the ground surface and the pipe is to allow for the increase in mean stress within the shearing zone during uplift. This stress increase leads to less dilatancy than would be implied by using the initial stress condition. The assumed value of p', combined with equations (6) and (7), allows peak angles of friction and dilation to be calculated, from which a value of peak uplift resistance can be found using equation (4). Lastly, a value for the at-rest earth pressure coefficient, K_0, must be adopted, and this has been taken as $(1 - \sin\phi_{\text{crit}})$, as is commonly assumed. The limit equilibrium solution then consists of equations (4)–(7) combined, such that

$$P = f(\gamma', Q, \phi_{\text{crit}}, I_D, H, D) \tag{8}$$

A complication of using Bolton's correlations is that uplift resistance P and overburden force $\gamma' HD$ are no longer in proportion, owing to the stress dependence of the peak angles of friction and dilation. Therefore design charts of N_γ against H/D, varying with ϕ_{crit}, must include multiple curves for varying relative density, bulk density and pipe diameter (hence ambient stress at a given H/D), as these parameters influence the relative dilatancy and peak friction angle. The

Table 1. Typical values of sand strength parameters (after Randolph *et al.*, 2004).

Sand mineralogy	Particle-crushing strength, $\log(\sigma'_c)$: σ'_c in kPa	Critical state friction angle, ϕ_{crit}: degrees
Quartz	10 ± 1	32·5 ± 1
Siliceous	10 ± 1	33 ± 1
Carbonate	8 ± 0·5	41 ± 1

Delivered by ICEVirtualLibrary.com to:
IP: 129.169.110.8
On: Tue, 02 Aug 2011 16:19:32

strength parameters Q and ϕ_{crit} show minimal variation between sands, so are not needed as further variables on generic design charts.

This limit equilibrium solution was presented by White *et al.* (2001) in terms of dilation angle rather than relative density. This approach of incorporating Bolton's correlations into an analytical solution to capture the influence of stress level and density on dilatancy and peak strength has been previously used by Randolph (1985) for pile base resistance. Graham & Hovan (1986) used a similar approach to derive design charts for shallow foundation capacity on soil with a stress and density-dependent friction angle.

During pipe or anchor uplift, the stress level within the failing soil is below the range of stresses over which equations (6) and (7) were originally validated using element test data. Tatsuoka (1987) and Bolton (1987) discuss triaxial test data which suggest that equations (6) and (7) are appropriate only for mean pressures greater than 150 kPa, although Fannin *et al.* (2005) show that the trends extend to lower stress levels. It is shown later that the accuracy of this solution appears to be independent of stress level, so it is not unreasonable to assume that the behaviour implied by Bolton's correlations continues to the lower stress levels relevant to pipe and anchor uplift.

COMPARISON WITH MODEL TEST DATABASE

A large database of pipe and anchor pullout tests has been collated, to test the reliability of the limit equilibrium solution for predicting pipe uplift resistance. As uplift of a continuous pipeline imposes nominally plane-strain conditions, only plate anchors with an aspect ratio (length divided by breadth) greater than 8 have been included. Results for rectangular plate anchors reported by Murray & Geddes (1987) and Rowe & Davis (1982) suggest that this aspect ratio is sufficient to eliminate end effects, thus simulating plane-strain conditions.

A total of 115 tests, all in silica sands, have been back-analysed for this paper. Details of each test series are given in Table 2. The database spans a wide range of relative densities (I_D = 10–92%, mean 43%) and embedment depths (H/D = 1 to 8, mean 4·24). Only tests at an embedment of $H/D \leqslant 8$ have been included. At high embedment depths, the failure mechanism changes to include localised flow around the pipe. Vanden Berghe *et al.* (2005) show that the depth of this transition depends on the dilatancy of the soil. This validation of the limit equilibrium solution is concerned only with embedments shallower than $H/D = 8$.

In most cases, sufficient information was provided by the original authors to allow the limit equilibrium solution to be applied. Where specific values have not been provided, soil strength parameters of $Q = 10$ and $\phi_{crit} = 32°$ have been assumed.

Figure 4 compares the measured values of normalised uplift resistance N_γ with the limit equilibrium solution, plotted for $\phi_{crit} = 32°$, and values of relative dilatancy I_R spanning the permissible range of 0 to 4. The appropriate version of equation (4) has been used in each case, accounting for the reduced volume of cover above a pipe. The database of results generally lies within the range of values predicted by the limit equilibrium solution, although there are significant outliers in loose conditions at high embedments. In these conditions a localised flow-round failure mechanism is likely to be optimal.

The predicted and measured values of peak uplift resistance are compared in Fig. 5, plotted against relative density, relative dilatancy, initial mean stress p' at pipe waist (or anchor level), and embedment depth. Although there is scatter, there is no significant skew with any of these

Table 2. Model test database of anchor and pipe uplift resistance

Authors	Test type	Centrifuge g-level	Sand	Pipe surface material	Dry or saturated	Number of tests	Cover depth ratio, H/D	Relative density, I_D: %	Relative dilatancy index, I_R
Barefoot (1998)	Pipe	20	Seabed sand	Aluminium	Saturated	7	4·6–6·2	40–70	3·2–4
Cheuk *et al.* (2007)	Pipe	–	Leighton Buzzard Sand Fractions A and D	Aluminium	Dry	4	3	30–92	1·6–4
Dickin (1988)	Anchor	40	Erith sand	Steel	Dry	15	1–8	33–76	0·8–4
Dickin (1994)	Pipe	40	Erith sand	Steel and sand coated	Dry	17	1·5–8	39–76	1–4
Matyas & Davis (1983)	Pipe	–	Sydney sand	Steel	Dry	8	2·7–8·8	21·9–59·4	1·1–4
Murray & Geddes (1987)	Anchor	–	Medium-grained sand	Steel and sand coated	Dry	3	3–6	85·9	4
Ng & Springman (1994)	Pipe	25–40	Leighton Buzzard Sand Fraction E	Aluminium	Saturated	3	4–4·1	43	2
Rowe & Davis (1982)	Anchor	–	Sydney sand	Steel	Dry	36	1–8	15–33	0·2–1·9
Trautmann *et al.* (1985)	Pipe	–	Cornell filter sand	Steel	Dry	10	1·5–8	10–78	0–4
White *et al.* (2001)	Pipe	10	Leighton Buzzard Sand Fraction D	Brass	Saturated	12	3·14	15·6–66·7	0·3–4

Delivered by ICEVirtualLibrary.com to:
IP: 129.169.110.8
On: Tue, 02 Aug 2011 16:19:32

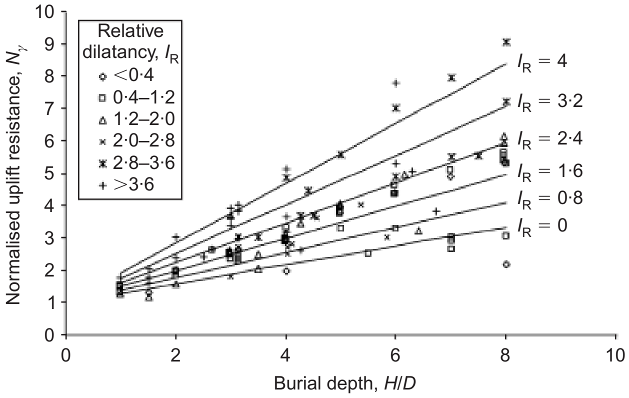

Fig. 4. Comparison of model test database and limit equilibrium solution

parameters, indicating that the influence of density and stress level on uplift resistance is broadly captured by the use of Bolton's correlations in the limit equilibrium solution. The mean ratio of predicted to measured peak uplift resistance of 1·00 is surprisingly accurate—misleadingly so, as noted below—and the coefficient of variation (COV) is 0·23.

This agreement is achieved without optimisation of the back-analysis, since the limit equilibrium solution contains no 'fitting' parameters. However, as with all studies of this kind, the level of agreement is dependent on the scope of the database: a future larger database, or a more selective smaller database, may not lead to the same accuracy.

Closer inspection of the database indicates that the 61 tests on model pipes show a mean overprediction of the peak uplift resistance by 11%, whereas the 54 tests on anchors show a mean underprediction of 14%. The overprediction on pipes is generally independent of embedment depth, but the underprediction of anchor capacity occurs mainly at deep embedments. These discrepancies may be (a) a feature of the database or (b) indicative of a systematic difference between the pipes and the strip anchors. Dickin (1994) conducted centrifuge tests on pipes and strip anchors in identical conditions and found no consistent difference. However, it was found that the uplift resistance of smooth pipes compared with rough was consistently lower by 10–30%, increasing with decreasing embedment. On the other hand, finite element results suggest that anchor plate roughness has negligible influence on the uplift resistance at all depths (Rowe & Davis, 1982).

A simple explanation for the contrast between pipes and anchors shown by the database is that most pipes within the database had a smooth surface (Table 2). Whereas the full soil strength can be mobilised in the region above a strip anchor (whether the anchor is smooth or rough), this is not the case at the surface of a smooth pipe. Therefore a smooth pipe is less able to transmit shear stress than the zone of soil above a strip anchor, which means less resistance can be mobilised on the lower part of the shear planes within the failure mechanism. At shallow embedments this weakening effect influences a larger proportion of the shear planes, explaining Dickin's higher discrepancy in shallower tests. Prototype pipelines, which usually have a rough coating, are less influenced by this effect, and so will mobilise a higher uplift resistance, closer to the predicted value and the response of a strip anchor. Model tests that intend to simulate a prototype case should use an appropriate pipe roughness.

An analogous influence of roughness exists for the deep penetration resistance of strip anchors and pipes—or piles and cylindrical penetrometers—in clay. The exact bearing capacity factor for a vanishingly thin buried strip anchor is 11·42, irrespective of roughness (Martin & Randolph 2001), whereas the resistance on a cylindrical object varies between 9·14 and 11·94 depending on roughness (Martin & Randolph 2006). This difference of 25% in the smooth case highlights

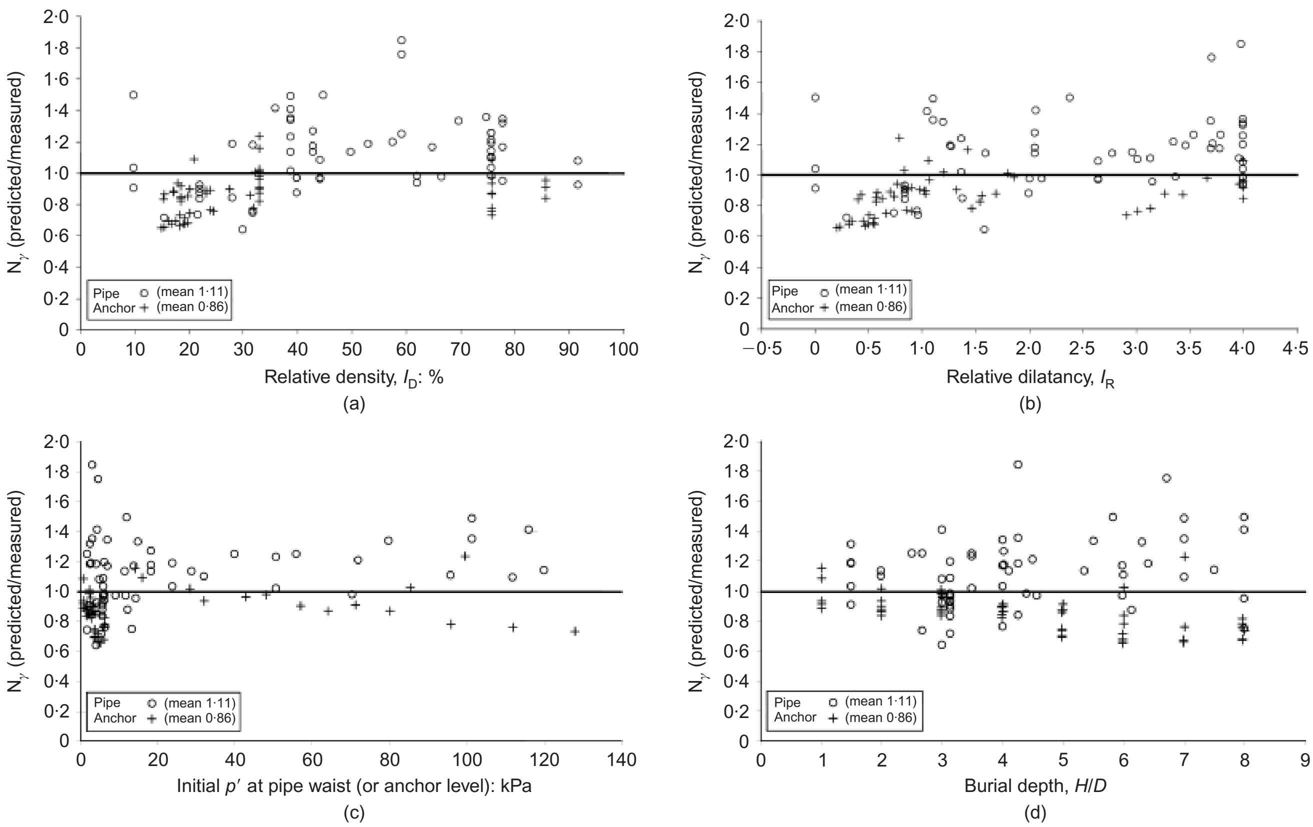

Fig. 5. Predicted against measured peak uplift resistance: (a) variation with relative density; (b) variation with relative dilatancy; (c) variation with mean stress, p'; variation with burial depth

Delivered by ICEVirtualLibrary.com to:
IP: 129.169.110.8
On: Tue, 02 Aug 2011 16:19:32

the weakening effect of a smooth pipe surface when compared with the behaviour of a strip anchor, and supports the explanation given previously for the contrast between pipes and anchors seen in the database.

COMPARISON WITH PLASTICITY SOLUTION

The peak uplift resistance predicted by this limit equilibrium solution is now compared with the plasticity solution given by equation (1), which has been verified as near optimal through finite element limit analysis reported by Merifield *et al.* (2001) and Merifield & Sloan (2006). Plasticity solutions require a single friction angle to be used, which is assumed to equal the dilation angle, following normality. If this value is taken as the peak friction angle (as might be assumed for finding peak uplift resistance) then equation (6) can be used to find an appropriate value of dilation angle for use in the limit equilibrium solution, for a given value of ϕ_{crit}. Fig. 6 shows that the plasticity solution based on peak friction angle predicts an uplift resistance higher by 50–70% than for the limit equilibrium solution. Given that the limit equilibrium solution is on average 14% lower than the database results for a rough strip, the discrepancy between the plasticity solution and the database is therefore an overprediction of 30–50%. A value of $\phi_{crit} = 32°$ has been used for this illustration, which is correct to within 2° for virtually all silica sands (Randolph *et al.*, 2004).

Alternatively, the plasticity solution might be applied using the critical state friction angle, in an attempt to be safely conservative. In this case, comparison can be made with the limit equilibrium solution by varying the relative dilatancy I_R (equation (7)) between the limits of 0 and 4 recommended by Bolton (1986). This variation covers the potential range of peak angles of friction and dilation. Fig. 7 shows that the plasticity solution is still unconservative compared with the limit equilibrium solution except in highly dilatant conditions, for which ϕ_{peak} exceeds 44°.

Given that the limit equilibrium solution captures the observed failure mechanism well and yields accurate predictions of uplift resistance (Fig. 5), these comparisons offer a means of verification (or otherwise) of the plasticity solution. Fig. 6 shows that the use of a peak angle of friction in the plasticity solution is likely to be unconservative, while the somewhat illogical use of a critical state friction angle to predict peak resistance can still be unconservative in conditions of low dilatancy (Fig. 7), as exhibited by loose soils or at deep embedment and hence high stress level.

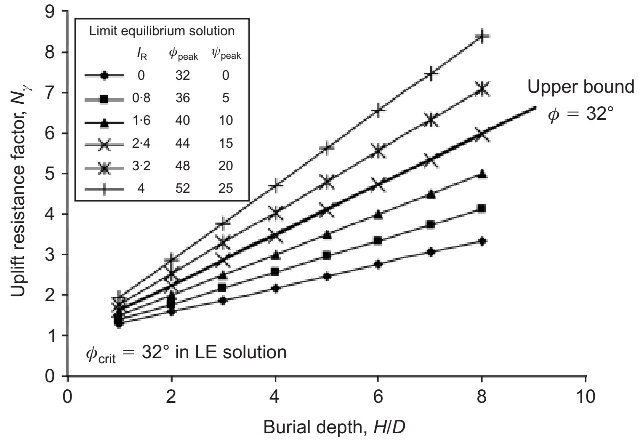

Fig. 7. Comparison of limit equilibrium and plasticity solutions, using ϕ_{crit} in both, but varying dilatancy in the LE solution

DESIGN CHARTS FOR PEAK UPLIFT RESISTANCE

By combining equations (3)–(7), the predicted peak uplift resistance factor N_γ, incorporating Bolton's stress–dilatancy relations, can be plotted as a function of normalised embedment H/D for a given combination of relative density I_D, effective unit weight γ', soil strength parameters ϕ_{crit} and Q, and the pipe diameter D.

Two such charts are shown in Fig. 8, considering two unit

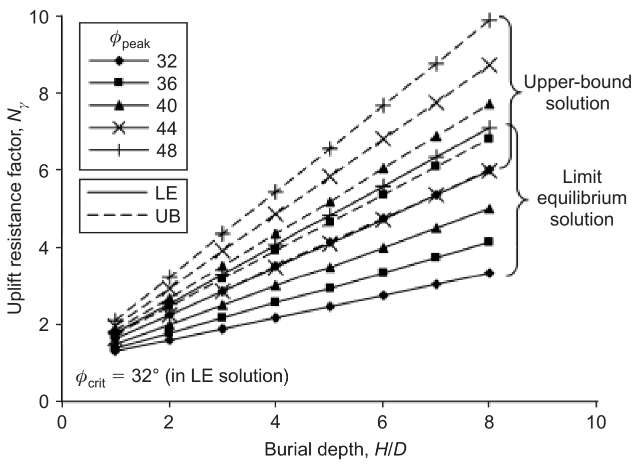

Fig. 6. Comparison of limit equilibrium and plasticity solutions, using ϕ_{peak} in both, but capturing dilatancy in the LE solution using ϕ_{crit} = 32°

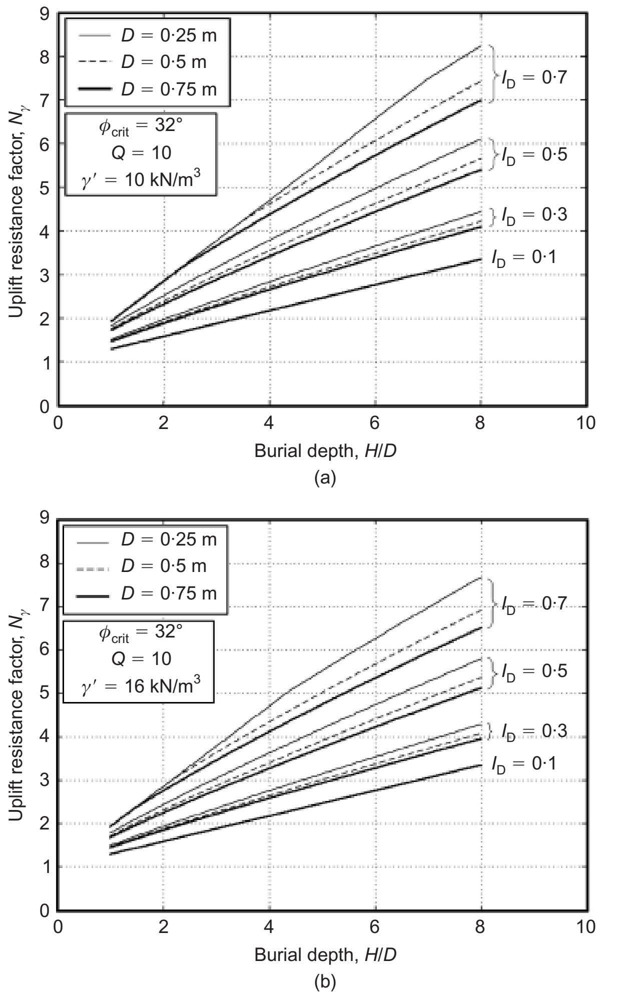

Fig. 8. Design charts for peak uplift resistance, N_γ against H/D: (a) submerged example ($\gamma' = 10$ kN/m³); (b) dry example ($\gamma' = 16$ kN/m³)

Delivered by ICEVirtualLibrary.com to:
IP: 129.169.110.8
On: Tue, 02 Aug 2011 16:19:32

weights of 16 and 10 kN/m^3, representing typical values in dry and submerged conditions, and using typical strength parameters, Q and ϕ_{crit}, for silica sands. Each chart shows curves corresponding to three pipe diameters and four values of relative density. For intermediate combinations of these variables interpolation can be used, or the exact uplift resistance can be calculated directly using equations (3)–(7).

The lines plotted in Fig. 8 are gently curved, reflecting the decrease in peak friction angle with increasing depth and hence stress level, as captured by equations (6) and (7). At very low embedments and high relative densities the curves for different pipe diameters overlie each other, as the advised upper limit on relative dilatancy of $I_R = 4$ is reached, imposing an upper limit on peak friction angle. Similarly, in very loose conditions, pipe diameter and effective unit weight have no effect on N_γ, as the lower limit on relative dilatancy of $I_R = 0$ is reached, and the peak friction angle is equal to the critical state value.

The form of Fig. 8 is not always amenable to use in design. Commonly, the pipe diameter and estimated values of the soil properties are known, while the cover depth H is to be determined. However, H affects both axes of Fig. 8, so an iterative approach is required to establish a design value. To eliminate the need for iteration, the limit equilibrium solutions are presented in an alterative way in Fig. 9. The predicted peak uplift resistance is normalised by $\gamma' D^2$ and plotted as a function of (H/D). This chart provides a more straightforward method for estimating uplift resistance.

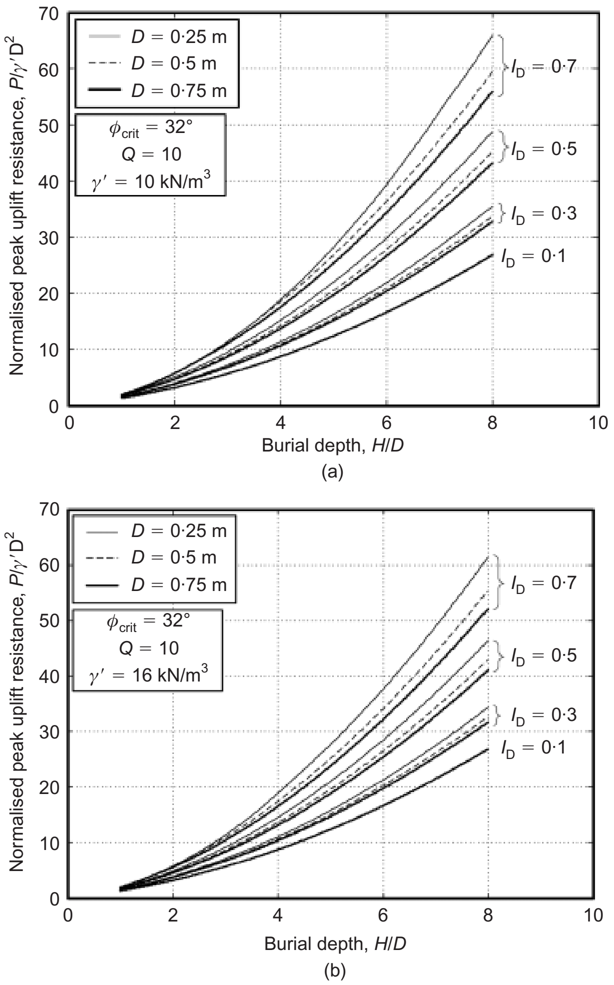

Fig. 9. Design charts for peak uplift resistance, $P\gamma'/D^2$ against H/D: (a) submerged example ($\gamma' = 10$ kN/m^3); (b) dry example ($\gamma' = 16$ kN/m^3)

APPLICATION TO DESIGN

This limit equilibrium solution offers a simple method for predicting the peak uplift resistance of buried pipelines and anchors. To apply this method in design, it is necessary to evaluate the following input parameters:

$$P = f(\gamma', \sigma_c, \phi_{crit}, I_D, H, D) \tag{8}$$

In silica and quartz sands the soil strength parameters $Q = \ln(\sigma_c)$ and ϕ_{crit} show minimal variation (Table 1), and in most onshore anchor applications the compaction of the backfill can be controlled to achieve the required design relative density I_D. For buried offshore pipelines the relative density of the cover material is dependent on the trenching and backfilling processes. Typical pipeline ploughs deposit backfill in a loose to medium dense state (Cathie *et al.*, 2005), although subsequent wave action can densify the backfill (Clukey *et al.*, 1989). In these loose conditions, it is important to account for the low dilatancy of the backfill. The comparison shown in Fig. 7 highlights the non-conservatism of the plasticity solution in these conditions. The limit equilibrium solution is more accurate, although a flow-round mechanism can be critical in very loose conditions and at high embedments (Vanden Berghe *et al.*, 2005).

As the backfilling of an offshore pipeline is difficult to control, it is useful to assess the relative density of the backfill in situ after construction. Puech & Foray (2002) describe the use of a miniature cone penetration tool to characterise seabed soils. The reduced size of a miniature cone allows improved interpretation at the shallow depths relevant to a trenched pipeline. Various empirical correlations exist for converting measurements of cone resistance into a value of relative density that can then be used in this limit equilibrium solution (when coupled with Bolton's correlations) (Jamiolkowski *et al.*, 2003; Schnaid, 2005).

CONCLUSIONS

Accurate prediction of the peak uplift resistance of buried pipes is critical to the safe design of buried offshore pipelines. Onshore structures and offshore vessels are also often restrained by the uplift resistance offered by buried anchors.

This paper describes a simple limit equilibrium solution for predicting the uplift resistance of pipes and plate anchors buried in sand. The geometry of this solution has been selected to match model test observations. Bolton's (1986) stress–dilatancy correlations are used to find peak angles of friction and dilation, establishing the geometry of the failure mechanism and the mobilised resistance. A database of 115 model tests on buried pipes and strip anchors has been assembled from the published literature to validate the solution. For the overall database, excellent agreement between the data and the limit equilibrium solution is shown, with an average ratio of predicted to measured uplift resistance of 1·00. However, for the database of pipes alone, the solution overpredicts resistance by an average of 11%. For strip anchors the resistance is underpredicted by an average of 14%. This discrepancy is attributed to the smooth surface of most model pipes, which prevents the transfer of shear stresses to the lower part of the failure planes. This bias will be reduced for prototype pipelines with a rough coating.

In contrast, it is shown that the solution for uplift resistance based on the limit theorems of plasticity is generally very unconservative. This non-conservatism can be attributed to the assumption of normality that is required by the limit theorems. Normality leads to unrealistically high dilation, which imposes an improbable uplift mechanism involving uplift of a far wider zone of soil than is seen in model tests. For this class of kinematically restrained problem, plasticity

Delivered by ICEVirtualLibrary.com to:
IP: 129.169.110.8
On: Tue, 02 Aug 2011 16:19:32

theory is an inappropriate tool for modelling the drained behaviour of soil.

The limit equilibrium solution has been used to produce simple design charts linking the peak uplift resistance to the normalised burial depth and to the critical state friction angle and relative density of the backfill.

REFERENCES

Barefoot, A. J. (1998). *Modelling the uplift resistance of buried pipes in a drum centrifuge*. MPhil thesis, Cambridge University Engineering Department.

Bolton, M. D. (1986). The strength and dilatancy of sands. *Géotechnique* **36**, No. 1, 65–78.

Bolton, M. D. (1987). Reply to discussion on 'The strength and dilatancy of sands'. *Géotechnique* **37**, No. 3, 225–226.

Cathie, D. N., Jaeck, C., Ballard, J.-C. & Wintgens J.-F. (2005). Pipeline geotechnics: state of the art. *Proceedings of the international symposium on frontiers in offshore geotechnics*, Perth, 95–114.

Cheuk, C. Y., White, D. J. & Bolton, M. D. (2007). Uplift mechanisms of pipes buried in sand. *J. Geotech. Geoenviron. Engng ASCE* **134**, No. 2, 154–163.

Clukey, E. C., Jackson, C. R., Vermersch, J. A., Koch, S. P. & Lamb, W. C. (1989). Natural densification of sand surrounding a buried offshore pipeline. *Proc. 21st Ann. Offshore Technol. Conf., Houston*, 291–300, Paper OTC6151.

Dickin, E. A. (1988). Uplift behaviour of horizontal anchor plates in sand. *J. Geotech. Engng ASCE* **114**, No. 11, 1300–1317.

Dickin, E. A. (1994). Uplift resistance of buried pipelines in sand. *Soils Found.* **34**, No. 2, 41–48.

Fannin, R. J., Eliadorani, A. & Wilkinson, J. M. T. (2005). Shear strength of cohesionless soil at low stresses. *Géotechnique* **55**, No. 6, 467–478.

Graham, J. & Hovan, J. M. (1986). Stress characteristics for bearing capacity in sand using a critical state model. *Can. Geotech. J.* **23**, No. 2, 195–202.

Jamiolkowski, M. B., Lo Presti, D. F. C. & Manassero, M. (2003). Evaluation of relative density and shear strength of sands from cone penetration test. In *Soil behaviour and soft ground construction,* ASCE Geotechnical Special Publication 119, pp. 201–238.

Martin, C. M. & Randolph, M. F. (2001). Applications of the lower and upper bound theorems of plasticity to collapse loads of circular foundations. *Proc. Int. Conf. on Computer Methods and Advances in Geomechanics*, Desai *et al.* (eds), 1417–1428.

Martin, C. M. & Randolph, M. F. (2006). Upper-bound analysis of lateral pile capacity in cohesive soil. *Géotechnique* **56**, No. 2, 141–145.

Matyas, E. L. & Davis, J. B. (1983). Experimental study of earth loads on rigid pipes. *J. Geotech. Engng, ASCE* **109**, No. 2, 190–201.

Merifield, R. S., Sloan, S. W., Abbo, A. J. & Yu, H. S. (2001). The ultimate pullout capacity of anchors in frictional soils. *Proc. 10th Int. Conf. on Computer Methods and Advances in Geomechanics, Tucson, AZ*, 1187–1192.

Merifield, R. S. & Sloan, S. W. (2006). The ultimate pullout capacity of anchors in frictional soils. *Can. Geotech. J.* **43**, No. 8, 852–868.

Murray, E. J. & Geddes, J. D. (1987). Uplift of anchor plates in sand. *J. Geotech. Engng ASCE* **113**, No. 3, 202–215.

Ng, C. W. W. & Springman, S. M. (1994). Uplift resistance of buried pipelines in granular materials. *Proc. Centrifuge '94, Singapore* **1**, 753–758.

Puech, A. & Foray, P. (2002). Refined model for interpreting shallow penetration CPTs in sands. *Proc. Offshore Technol. Conf., Houston*, Paper OTC14275.

Randolph, M. F. (1985). *Capacity of piles driven into dense sand*, Technical Report CUED/D-SOILS/TR171. Cambridge: Cambridge University Engineering Department.

Randolph, M. F., Jamiolkowski, M. B. & Zdravkovic, L. (2004). Load carrying capacity of foundations. *Proc. Skempton Memorial Conf., London* **1**, 207–240.

Rowe, P. W. (1962). The stress–dilatancy relation for static equilibrium of an assembly of particles in contact. *Proc. R. Soc. London Ser. A* **269**, 500–527.

Rowe, P. W. (1969). The relation between the shear strength of sands in triaxial compression, plane strain and direct shear. *Géotechnique* **19**, No. 1, 75–86.

Rowe, R. K. & Davis, E. H. (1982). Behaviour of anchor plates in sand. *Géotechnique* **32**, No. 1, 25–41.

Schnaid, F. (2005). Geocharacterisation and properties of natural soils by in-situ tests. *Proc. 16th Int. Conf. Soil Mech. Found. Engng, Osaka* **1**, 3–45.

Tatsuoka, F. (1987). Discussion on 'The strength and dilatancy of sands'. *Géotechnique* **37**, No. 3, 219–225.

Trautmann, C. H., O'Rourke, T. D. & Kulhawy, F. H. (1985). Uplift force–displacement response of buried pipe. *J. Geotech. Engng ASCE* **111**, No. 9, 1061–1076.

Vanden Berghe, J. F., Cathie, D. & Ballard, J. C. (2005). Pipeline uplift mechanisms using finite element analysis. *Proc. 16th Int. Conf. Soil Mech. Found. Engng, Osaka* **3**, 1801–1804.

Vermeer, P. A. & Sutjiadi, W. (1985). The uplift resistance of shallow embedded anchors. *Proc. 11th Int. Conf. Soil Mech. Found. Engng, San Francisco* **3**, 1635–1638.

White, D. J., Barefoot, A. J. & Bolton, M. D. (2001). Centrifuge modelling of upheaval buckling in sand. *Int. J. Phys. Modelling Geomech.* **2**, 19–28.

White, D. J., Take, W. A. & Bolton, M. D. (2003). Soil deformation measurement using particle image velocimetry (PIV) and photogrammetry. *Géotechnique* **53**, No. 7, 619–631.

Delivered by ICEVirtualLibrary.com to:
IP: 129.169.110.8
On: Tue, 02 Aug 2011 16:19:32